

Production of Brewster angle thin film polarizers using a $\text{ZrO}_2/\text{SiO}_2$ pair of materials

V. ZHUPANOV,¹ I. KOZLOV,² V. FEDOSEEV,¹ P. KONOTOPOV,¹ M. TRUBETSKOV,^{2,3} AND A. TIKHONRAVOV^{2,*}

¹Scientific Research Institution "Lutch," Zeleznodorozhnaya 24, Podolsk, Moscow, Russia

²Research Computing Center, Moscow State University, Leninskie Gory, 119992 Moscow, Russia

³Max-Planck Institute of Quantum Optics, Hans-Kopfermann str. 1, 85748 Garching, Germany

*Corresponding author: tikh@srcc.msu.ru

Received 29 July 2016; revised 9 October 2016; accepted 10 October 2016; posted 10 October 2016 (Doc. ID 272701); published 7 November 2016

The production of polarizers for high-intensity applications based on a $\text{ZrO}_2/\text{SiO}_2$ pair of thin film materials is discussed. A special approach to accurate determination of a ZrO_2 refractive index and the application of direct broadband optical monitoring enable obtaining good manufacturing results. © 2016 Optical Society of America

OCIS codes: (310.0310) Thin films; (310.4165) Multilayer design; (310.1860) Deposition and fabrication.

<http://dx.doi.org/10.1364/AO.56.000C30>

1. INTRODUCTION

Multilayer polarizers are among the key thin film elements required for fusion laser optics [1–3]. High-fluence thin film material combinations such as $\text{ZrO}_2/\text{SiO}_2$ and $\text{HfO}_2/\text{SiO}_2$ have been discussed as material pairs for these elements with the most potential [4]. Until now, most publications in this area have been connected with production of polarizers using the second pair of materials [2,3,5–8]. At the same time, the pair $\text{ZrO}_2/\text{SiO}_2$ has a higher index contrast and thus, according to the maximum principle in thin film optics [9], enables obtaining better polarizer designs with a smaller number of design layers.

Another advantage of using ZrO_2 as a high index material is its much lower cost compared with HfO_2 . On the other hand, there are serious difficulties connected with using ZrO_2 . In the first turn, they are connected with optical and crystalline inhomogeneity of ZrO_2 films [10]. As a result, the refractive index of ZrO_2 is very much dependent not only on the deposition conditions but also on the thickness of a deposited film.

Spectral properties of Brewster angle thin film polarizers are quite sensitive to production errors [6,8], and the reliable monitoring of coatings layers' thickness is crucial for successful production. In [6,8], combinations of various monochromatic optical monitoring techniques with quartz crystal monitoring were applied for the production of $\text{HfO}_2/\text{SiO}_2$ Brewster angle polarizers. Broadband optical monitoring strategies have attracted greater attention recently in connection with the production of optical coatings of various types [11]. It has been shown that for several types of optical coatings, direct broadband optical monitoring provides an error self-compensation effect that can be rather strong for specific coating designs [12]. It is interesting to investigate the prospects for direct broadband

optical monitoring in connection with production of Brewster angle polarizers.

In this paper, the design and production of $\text{ZrO}_2/\text{SiO}_2$ Brewster angle polarizers for wavelengths of 1064 nm are considered. The main challenge connected with using $\text{ZrO}_2/\text{SiO}_2$ as a pair of polarizer materials is the reliable determination of the refractive index of ZrO_2 . This topic is discussed in Section 2. Section 3 is devoted to the applied direct broadband optical monitoring approach. It also presents manufacturing results. Conclusions are summarized in Section 4.

2. CHARACTERIZATION AND THEORETICAL DESIGNS

As shown in [10], e-beam evaporated ZrO_2 thin films are crystallographically inhomogeneous. With their growth they feature monoclinic and then cubic phases. These conclusions have been supported by our own investigations. In this work, results for ion-assisted e-beam evaporation are presented. The samples discussed below have been deposited at $2 \cdot 10^{-6}$ millibar residual pressure on substrates at room temperature with 200 μA ion current density.

It has been found that the growing film is first amorphous, and then crystalline phases start to develop. Because of this fact, ZrO_2 films with different thicknesses may have different refractive indexes. Accurate knowledge of the actual refractive indexes of deposited films is important not only for the design of optical coatings but also for the monitoring of deposition processes if optical monitoring techniques are applied. Therefore, accurate optical characterization of ZrO_2 films is extremely important.

For accurate determination of the ZrO_2 refractive index, the previously developed experimental approach [13] is applied. First, samples with relatively thick ZrO_2 layers are deposited,

measured, and accurately characterized using the OptiChar module of the OptiLayer thin film software [14]. After this, a special quarter wave mirror with layer thicknesses close to those of the planned polarizer design is deposited. Its spectral characteristic in the spectral region covering the planned monitoring spectral region is measured, and the OptiRE module of the OptiLayer software [14] is applied for more accurate determination of ZrO₂ refractive index.

The red solid curve in Fig. 1 shows the ZrO₂ refractive index found from reflectance measurement data for the single film sample having a physical thickness of 368 nm. ZrO₂ layers in polarizer designs are expected to be three times thinner and due to this fact may have different refractive indexes. This is indeed confirmed by the test deposition of the 14-layer quarter wave mirror with a central wavelength of 1064 nm. Crosses in Fig. 2 show measured transmittance of this mirror. One can see that the actual width of the high reflection zone is noticeably narrower than the theoretically expected width—the solid curve in Fig. 2 presents the theoretically calculated transmittance of this mirror. The width of the high reflection zone is directly related to the ratio of mirror high and low refractive indexes. Indexes of SiO₂ films are stable, and one should

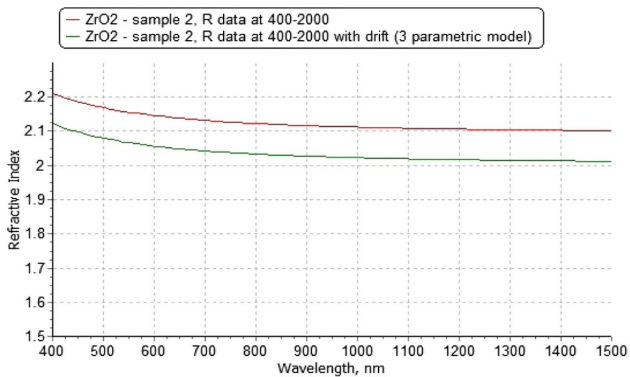


Fig. 1. Refractive index of ZrO₂ before (red curve) and after (green curve) correction using the reverse engineering of the 14-layer quarter wave mirror.

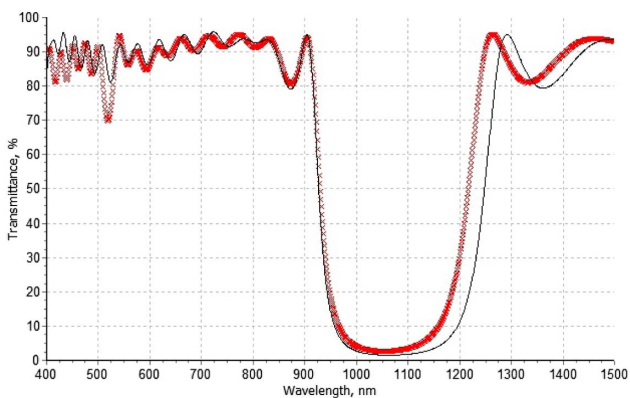


Fig. 2. Initial fitting of the measured reflectance of the 14-layer quarter wave mirror (crosses) by the theoretical reflectance of this mirror (solid curve).

attribute the observed difference between the two curves in Fig. 2 to the variation of the ZrO₂ refractive index from the specified dependence.

The wavelength dependence of the ZrO₂ refractive index (the red curve in Fig. 1) has been verified against well-known and well-trusted dependencies of the ZrO₂ refractive index from several sources. For this reason, for the reverse engineering of measurement data in Fig. 2, the OptiRE model assuming drift of the found refractive index upward or downward is applied. We also assume that there could be systematic errors in thicknesses of high and low index layers; that is, all high index layer thicknesses and all low index layer thicknesses may differ from respective nominal thicknesses by some percentage values (relative errors of high and low index layers). Thus our reverse engineering model has three unknown parameters: drift of ZrO₂ index and relative errors of high and low index layers. After the application of the reverse engineering fitting procedure, an excellent correspondence between measured and model transmittance data is achieved (not shown in Fig. 2). The corrected ZrO₂ refractive index is presented by the green curve in Fig. 1.

Using the refined ZrO₂ refractive index, several polarizer theoretical designs for wavelengths of 1054 and 1064 nm with numbers of layers ranging from 28 to 32 have been obtained. Layer optical thicknesses of the 28-layer polarizer design for the 1064 nm wavelength are shown in Fig. 3. At the angle of incidence equal to 55.6 deg, this design provides transmittance for the *p*-polarized light T_p higher than 98% and transmittance for the *s*-polarized light T_s lower than 1% in the spectral region with the 28.8 nm width.

3. MONITORING AND MANUFACTURING RESULTS

Brewster angle polarizers have been produced for wavelengths of 1054 and 1064 nm on the substrates with dimensions of up to 430 by 750 mm. In this section, monitoring and manufacturing results are presented for the test sample with a working wavelength of 1064 nm. This test sample has been deposited on the BK7 substrates with 40 mm diameters in the Leybold-1100 vacuum chamber equipped with a cryogenic pump using

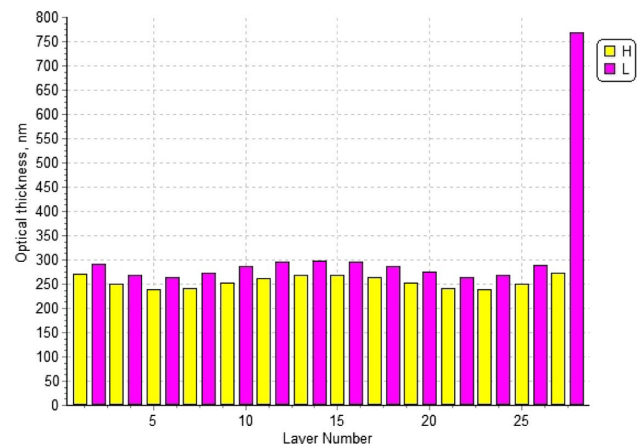


Fig. 3. Layer optical thicknesses of the 28-layer Brewster angle polarizer design for the 1064 nm wavelength.

e-beam evaporation with oxygen ions' assistance. The starting material for SiO_2 layers' deposition is the composite of quartz granules, while for ZrO_2 layers' deposition metallic zirconium is used. To control the stability of evaporation rates, quartz crystal monitoring is applied.

Monitoring of the thickness of deposited layers is performed with a broadband monitoring system, including an Avantes AvaSpec-2048XL spectrophotometer and several devices assisting measurements directly on one of the samples placed on a rotating substrate holder. Calibration of the monitoring system and direct transmittance measurements on the selected sample are performed at each rotation of the substrate holder. The calibration is based on 0% and 100% transmittance measurements at certain angular positions of the substrate holder (100% measurements performed when a hole of the substrate holder passes the spectrophotometer beam). For accurate determination of the angular positions of the rotating substrate holder, the Renishaw absolute position optical encoder is used. The card NI PCI-7811R with FPGA and specially developed software is used to control the whole process of measurements, including preliminary processing of data (averaging, smoothing, calibration).

Normal incidence broadband transmittance spectra are acquired at 2036 spectral points in the wavelength region from 658 to 1172 nm. This region covers the polarizer working wavelength of 1064 nm, but the polarizer working angle of incidence is different, and polarizer spectral properties are not directly seen in measured transmittance spectra. This section presents results obtained using this approach.

The deposited sample discussed in this section is not the best among the obtained results. It is selected to vividly demonstrate the most important features of the applied monitoring approach. Figure 4 illustrates the situation at the end of deposition of the first layer of this sample. One can observe a noticeable discrepancy between theoretical and measured transmittance curves at the end of the first layer deposition. Our monitoring device is accurately calibrated before acquisition of each new transmittance spectra, and linearity of the used monitoring scheme has been verified and confirmed. So the observed discrepancy cannot be attributed to systematic errors in measurement data. The main reason for the observed discrepancy is a drift of the refractive index of the first ZrO_2 layer

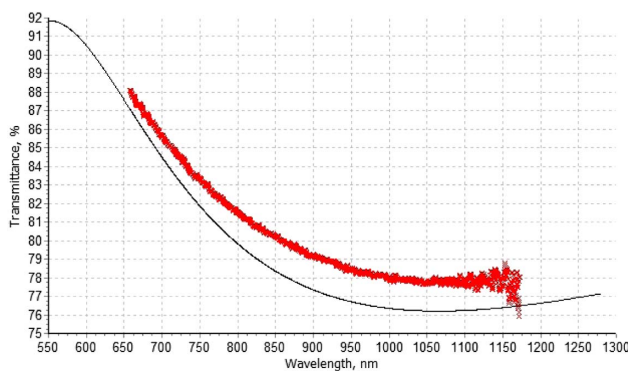


Fig. 4. Correspondence between theoretical and measurement data at the end of first layer deposition: noticeable discrepancy is caused by the variation of refractive index of the first ZrO_2 layer.

from the nominal refractive index wavelength dependence specified for designing and monitoring (see Section 2). In the applied monitoring approach, terminations of layer depositions are done not according to the minimum of the discrepancy functional but according to the correspondence of wavelength positions of extrema of measured and theoretical transmittance curves [13]. For the first layer, this provides an accurate control of its optical thickness because the wavelength position of transmittance minimum in Fig. 4 is directly related to this parameter.

Figure 5 shows the correspondence between measured and theoretical transmittance curves at the end of deposition of the last 28th layer. For other layers from 2 to 27, correspondences between measured and theoretical spectra are typically better than those shown in Figs. 4 and 5. Broadband optical monitoring spectra recorded at the ends of depositions of all polarizer layers provide enough information for the reverse engineering of the produced sample using various models, assuming both thickness and refractive index errors. For reverse engineering data processing, the OptiRE module of the OptiLayer software [14] has been applied.

Figure 6 presents the relative errors in thickness of polarizer layers found with the OptiRE model, assuming random errors

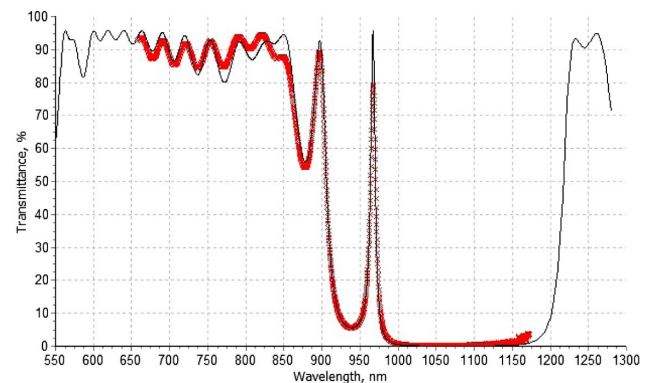


Fig. 5. Correspondence between theoretical and measurement data at the end of deposition of the last 28th sample layer.

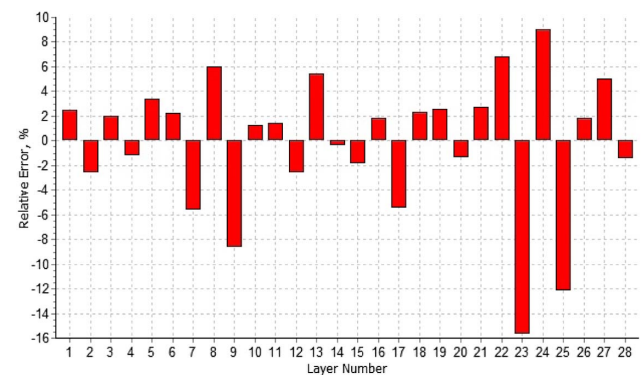


Fig. 6. Thickness errors found by the reverse engineering of 28 monitoring spectra recorded at the ends of layer depositions—model with random errors in all layer thicknesses and drift of the first layer refractive index is applied.

in the thicknesses of coating layers and drift of the first layer refractive index [14]. The relative drift of the first layer index is -1.72% . In the frame of this model, an excellent fit of measured data shown in Fig. 4 is achieved. The reverse engineering attempt with the other model, assuming drifts of all high and low refractive indexes, doesn't allow one to improve fitting of measured data. It gives thickness errors close to those shown in Fig. 6. At the same time, this model doesn't provide a good fit of measured data for the first coating layer. On the whole, the above facts confirm that for the considered sample there is a noticeable variation of the first layer index. Of course there could be some variations of the refractive indexes of other coating layers, but they are much less essential than the variation of the first layer index.

The main problem associated with direct optical monitoring techniques is the development of the cumulative effect of thickness errors with the growing number of deposited layers [15]. This effect is clearly observed in Fig. 6. Relative errors become really high for layers 23 and 25. With thickness errors at such a level, one should expect a total failure of spectral properties for the discussed polarizer sample. But, incredibly, spectral properties of this sample are in fact very good. Figure 7 presents measured s - and p -transmittances of the deposited sample at 55.6 deg of light incidence. At 1064 nm, T_p is equal to 98.2% and T_s is equal to 0.6% . Respective values for the theoretical design are 99.98% and 0.73% .

All direct optical monitoring techniques cause a correlation of errors in the thickness of deposited layers. The cumulative effect of thickness errors is a consequence of this correlation. But along with this negative effect, a correlation of thickness errors may also produce a positive effect known as a self-compensation of thickness errors [11,12]. Results presented in Fig. 7 allow one to suppose that the strong error self-compensation effect is observed when Brewster angle polarizers are produced using direct broadband optical monitoring. To confirm this statement, we performed a series of simulation experiments with noncorrelated thickness errors for the same polarizer design as above. Errors in layer thicknesses are simulated using Gaussian distribution of thickness errors with zero mathematical expectations and standard deviations equal to the modulus of thickness errors presented in Fig. 6. The results of simulation experiments are averaged over 1000 tests

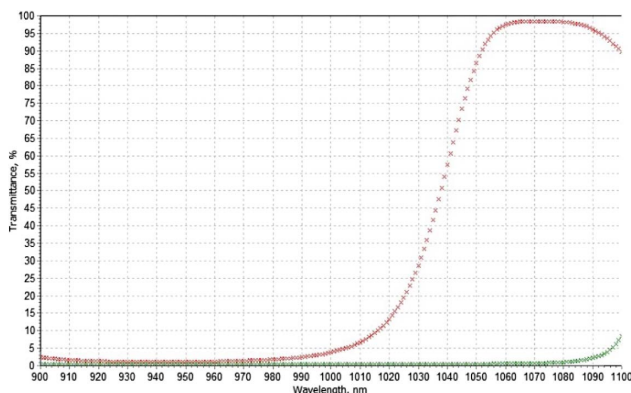


Fig. 7. Measured s - and p -transmittances for the sample with thickness errors presented in Fig. 6.

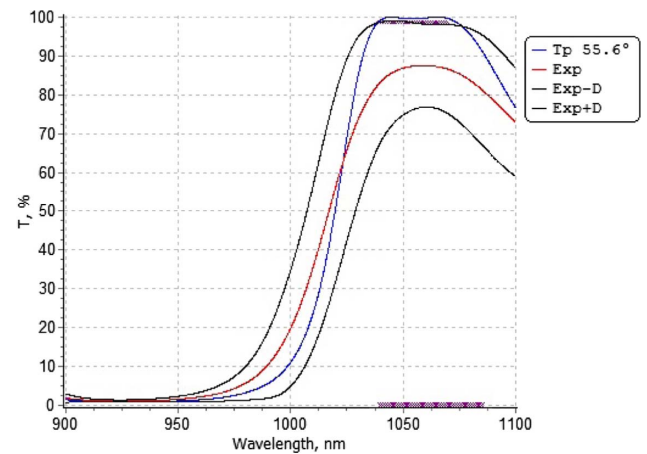


Fig. 8. Mathematical expectation (red curve) and corridor of standard deviations (black curves) for the p -transmittance calculated based on a series of simulation experiments with noncorrelated thickness errors having the same levels as the levels of error shown in Fig. 6. Blue curve is the theoretical p -transmittance.

with such errors. Figure 8 presents the mathematical expectation and the corridor of standard deviations for the calculated p -transmittance. One can see that in the case of noncorrelated thickness errors with the same average levels as the levels of error in Fig. 6, spectral properties of the polarizer in the p -polarized light are entirely destroyed. This confirms the presence of a strong error self-compensation effect in the case of polarizer production with layer thickness control by direct broadband optical monitoring.

4. CONCLUSION

The described direct broadband optical monitoring approach has been applied to production of Brewster angle polarizers with higher geometrical dimensions in other deposition chambers. Excellent manufacturing results for samples with dimensions of up to 430 by 750 mm have been obtained. We attribute the success of deposition with broadband optical monitoring to the existence of a strong error self-compensation effect associated with this type of monitoring. The existence of this effect has been demonstrated by presenting manufacturing results for the sample with high levels of thickness errors. Typically, production errors are several times lower and manufacturing results are better than those discussed in this paper.

For successful application of broadband optical monitoring strategies, accurate knowledge of actual refractive indexes of deposited thin films in the monitoring spectral region is important. A special approach based on the combination of characterization and reverse engineering procedures allows us to determine the ZrO_2 refractive index with sufficient accuracy, and this opens the way to production of Brewster angle polarizers with the ZrO_2/SiO_2 pair of thin film materials.

Funding. Russian Foundation for Basic Research (RFBR) (16-07-00872a); Deutsche Forschungsgemeinschaft (DFG) Cluster of Excellence; Munich-Centre for Advanced Photonics (MAP).

Acknowledgment. The authors are grateful to Markus Schulz from Agilent Technologies for accurate measurements of samples' spectral characteristics.

REFERENCES

1. C. J. Stolz, "Brewster's angle thin film plate polarizer design study from an electric field perspective," *Proc. SPIE* **3738**, 347–353 (1999).
2. C. J. Stolz, "Status of NIF mirror technologies for completion of the NIF facility," *Proc. SPIE* **7101**, 710115 (2008).
3. J. B. Oliver, A. L. Rigatti, J. D. Howe, J. Keck, J. Szczepanski, A. W. Schmid, S. Papernov, A. Kozlov, and T. Z. Kosc, "Thin film polarizers for the OMEGA EP laser system," *Proc. SPIE* **5991**, 599119 (2005).
4. C. Fournet, B. Pinot, B. Geenen, F. Ollivier, and W. Alexandre, "High damage threshold mirrors and polarizers in the ZrO_2/SiO_2 and HfO_2/SiO_2 dielectric systems," *Proc. SPIE* **1624**, 282–293 (1991).
5. C. J. Stolz, F. Y. Genin, T. A. Reitter, N. Molau, R. P. Bevis, M. K. von Gunten, D. J. Smith, and J. F. Anzellotti, "Effect of SiO_2 overcoat thickness on laser damage morphology of HfO_2/SiO_2 Brewster's angle polarizers at 1064 nm," *Proc. SPIE* **2966**, 265–272 (1997).
6. M. Zhu, K. Yi, W. Zhang, Z. Fan, H. He, and J. Shao, "Preparation of high performance thin-film polarizers," *Chin. Opt. Lett.* **8**, 624–626 (2010).
7. M. Zhu, K. Yi, Z. Fan, and J. Shao, "Theoretical and experimental research on spectral performance and laser induced damage of Brewster's thin film polarizers," *Appl. Surf. Sci.* **257**, 6884–6888 (2011).
8. J. Zhang, Y. Xie, X. Cheng, T. Ding, and Z. Wang, "Broadband thin-film polarizers for high-power laser systems," *Appl. Opt.* **52**, 1512–1516 (2013).
9. A. V. Tikhonravov, "Some theoretical aspects of thin film optics and their applications," *Appl. Opt.* **32**, 5417–5426 (1993).
10. R. E. Klinger and C. K. Carniglia, "Optical and crystalline inhomogeneity in evaporated zirconia films," *Appl. Opt.* **24**, 3184–3187 (1985).
11. A. Tikhonravov, M. Trubetskov, and T. Amotchkina, "Optical monitoring strategies," in *Optical Thin Films and Coatings: from Materials to Applications*, A. Piegari and F. Flory, eds., Woodhead Publishing Series in Electronic and Optical Materials (Cambridge, 2013), p. 864.
12. A. Tikhonravov, M. Trubetskov, and T. Amotchkina, "Investigation of the error self-compensation effect associated with broadband optical monitoring," *Appl. Opt.* **50** (9), C111–C116 (2011).
13. V. Zhupanov, V. Fedoseev, M. Trubetskov, T. Amotchkina, and A. Tikhonravov, "Design and production of three line antireflection coating for visible—far infrared spectral regions," *Proc. SPIE* **9627**, 962706 (2015).
14. A. Tikhonravov and M. Trubetskov, OptiLayer Software, <http://www.optilayer.com>.
15. A. Tikhonravov, M. Trubetskov, and T. Amotchkina, "Investigation of the effect of accumulation of thickness errors in optical coating production using broadband optical monitoring," *Appl. Opt.* **45**, 7026–7034 (2006).